

# An audio frequency filter application of micromachined thermally-isolated diaphragm structures

Kwang-Hyun Lee<sup>a,\*</sup>, Hyung-Kew Lee<sup>a</sup>, Hee-Jin Byun<sup>a</sup>, Il-Joo Cho<sup>a</sup>,  
Jong-Uk Bu<sup>b</sup>, Euisik Yoon<sup>a</sup>

<sup>a</sup>Department of Electrical Engineering, Korea Advanced Institute of Science and Technology (KAIST), 373-1,  
Kusong-dong, Yusong-gu, Taejon, South Korea

<sup>b</sup>LG Corporate Institute of Technology, 16 Woomyeon-dong, Seocho-gu, Seoul 137-724, South Korea

## Abstract

This paper reports a new application of micromachined thermally-isolated diaphragm structures for audio frequency filters. A pair of electrothermal elements that consist of a heater and a temperature sensor integrated in the same dielectric diaphragm have been used as a basic filter component. The electrothermal response of the diaphragm structure has one-pole, low-pass filtering characteristics. Various filter configurations using the fabricated electrothermal structures with driving circuitry have been tested. Measured responses of the filters show that cut-off frequencies can be electrically tuned, ranging from 30 to 300 Hz. Design parameters and guidelines have been identified and analyzed with respect to filter characteristics. The results have demonstrated the possibility that the thermally-isolated diaphragm structures can be used for audio frequency filter applications. © 2001 Elsevier Science B.V. All rights reserved.

*Keywords:* Micromachining; Electrothermal structure; Diaphragm; Filter; Audio frequency

## 1. Introduction

Previously, micromachined electrothermal structures were used for mass flow sensors, rms-dc converters, infrared sensors [1–4] etc. These applications take advantage of the thermal properties of the structures: low thermal conductance allowing effective sensing of small temperature changes in flow sensors and infrared sensors; and large thermal capacitance filtering out high frequency signals in rms-dc converters. Generally, micromachined structures can give these desirable characteristics implemented by IC compatible processes in a small size. In this paper, we have demonstrated the filter applications of the micromachined electrothermal structure in the audio frequency range with driving circuitry.

Typically, audio-band electrical filters have been implemented using Gm-C or switched capacitor techniques. However, they have some drawbacks. Gm-C filters require large capacitors and low-gain transconductors while switched capacitor filters have high switching noise and alias effects. It has been reported that the realization of audio frequency range filters becomes much easier and simple by using the

large effective time constant that can be obtained in temperature domain [5,6]. In the previous approaches, the bulk silicon has been used as a thermal structure. This makes the filter bulky, consume large power, and difficult to control thermal characteristics. Large thermal conductivity of the bulk structure requires large electrical power to raise the temperature in the structure. The thermal interactions between sensors and heaters on the bulk silicon complicate the analysis of thermal characteristics.

We report on micromachined electrothermal structures that are easy to customize the thermal characteristics. The fabrication process flow of these structures and the basic principles of filter operation using electrothermal components will be described. Experimental results on thermal characteristics of the structure and filter operations will be given, followed by the discussion of design factors and basic considerations for optimizing design parameters in audio frequency filter applications using the micromachined electrothermal structures.

## 2. Fabrication process

Fig. 1 shows the fabrication process flow of the electrothermal diaphragm structures. It consists of a thin diaphragm for thermal isolation and two metal resistors as a sensor and

\* Corresponding author. Tel.: +82-42-869-8062; fax: +82-42-869-3410.  
E-mail address: khlee@iml.kaist.ac.kr (K.-H. Lee).

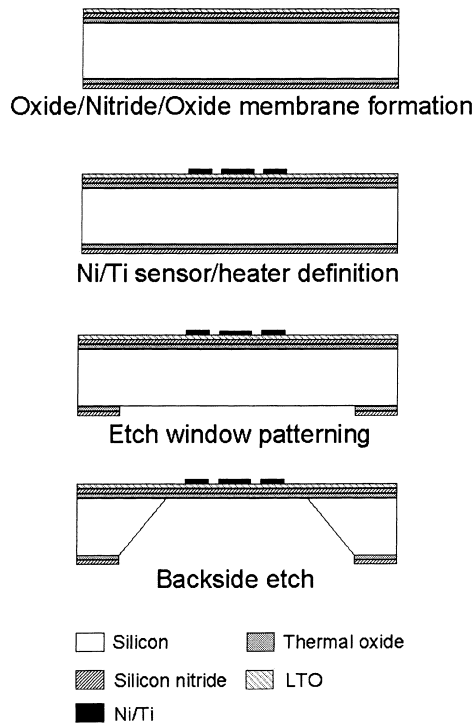


Fig. 1. Fabrication process flow.

a heater. The membrane has been fabricated using a silicon oxide/silicon nitride/silicon oxide multi-layer film. First, thermal silicon oxide is grown followed by the deposition of silicon nitride by LPCVD. Low temperature oxide (LTO) is deposited as the third layer of the membrane. The heater and sensor resistors are deposited and patterned by lift-off technique. We have used nickel for the metal resistors with titanium as an adhesion layer. Each layer has thicknesses of 400 and 100 Å, respectively. Temperature coefficient of resistance (TCR) of the metal resistor has been measured as 0.24%/K. Finally, etch window is defined in the backside followed by anisotropic silicon etch in 25% KOH at 85°C for 7 h. The fabricated electrothermal structures are shown in

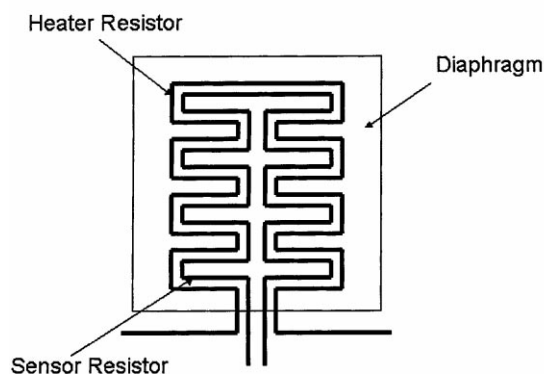


Fig. 2. Microphotographs of the fabricated thermally-isolated diaphragm structures.

Fig. 2. Typically, they have a diaphragm size of  $500 \mu\text{m} \times 500 \mu\text{m}$ , sensor resistance of  $3 \text{ k}\Omega$ , heater resistance of  $1.7 \text{ k}\Omega$ , and thermal conductance of about  $1.5 \times 10^{-4} \text{ W/K}$ , respectively.

### 3. Principle of filter operation

Fig. 3 shows the principle of filter operation using the electrothermal structures. A sinusoidal signal superimposed with dc bias level is applied to the heating resistor and the temperature variation of the sensor resistor is converted into an electrical output signal. The temperature of the diaphragm cannot respond as fast as the variation of the input sinusoidal signal because of thermal mass, i.e. filtering out high frequency components. We can represent the thermal interactions in the diaphragm structure as the following differential equation:

$$C_{\text{th}} \frac{d\Delta T}{dt} + G_{\text{th}} \Delta T = \Phi \quad (1)$$

where  $G_{\text{th}}$  and  $C_{\text{th}}$  are thermal conductance and thermal capacitance of the structure,  $\Delta T$  temperature variation of the structure and  $\Phi$  the heater power supplied to the structure, respectively. Analogically, the thermal characteristics of the diaphragm structure can be viewed as the equivalent electrical RC network as shown in Fig. 3. We have tested the frequency response of the electrothermal structure. The sinusoidal voltage was applied to the heater with a bias offset and the voltage variation of the sensor resistor was measured. Quiescent bias power must be applied to the electrothermal structure through a heater in order to maintain the signal integrity in the thermal domain. Fig. 4 shows the square pulse response of the electrothermal structure confirming its low-pass filter operation. Fig. 5 shows the measured thermal transfer function characteristics of the structure. It shows dominant one-pole, low-pass characteristics with a time constant of 9.8 ms.

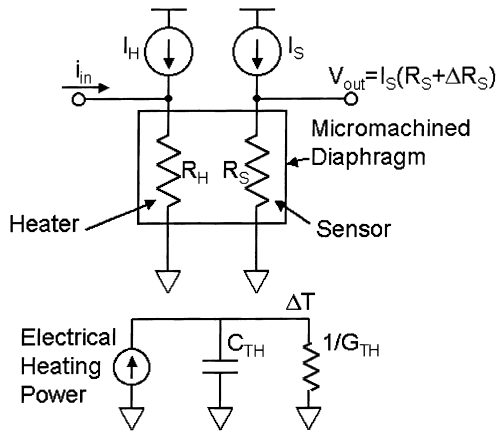


Fig. 3. Principle of filter operation in the electrothermal structure.

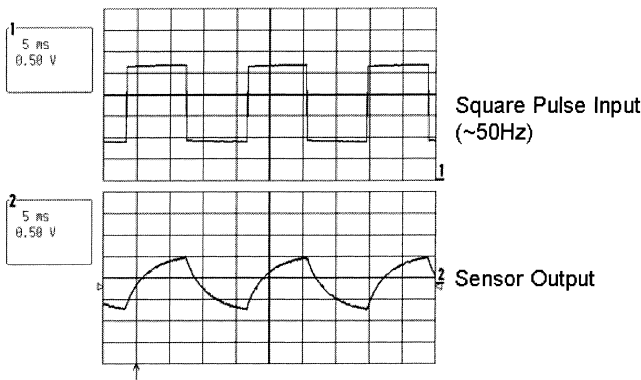


Fig. 4. Square pulse response of the electrothermal structure.

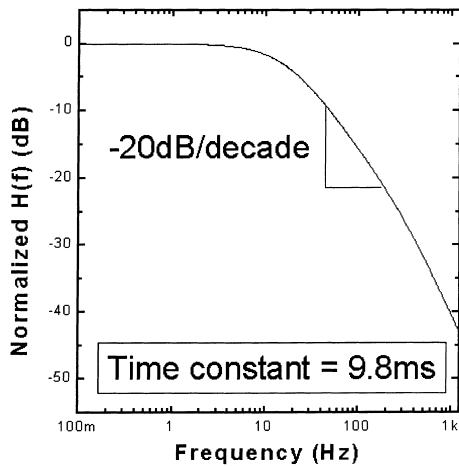


Fig. 5. Typical measured thermal characteristics of the diaphragm structure.

**4. Filter design**

We can make an integrator using the electrothermal structures with driving circuitry, which is equivalent to an electrical Gm-C integrator as shown in Fig. 6. The tempera-

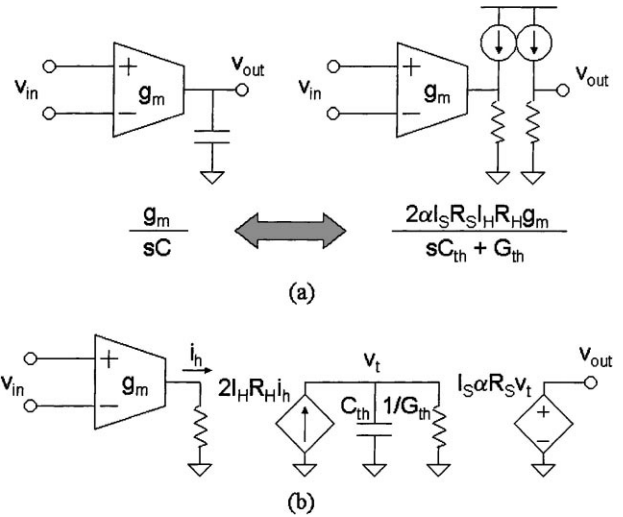


Fig. 6. (a) Analogy between electrical Gm-C integrator and electrothermal integrator. (b) Detailed equivalent circuits of electrothermal integrator.

ture of diaphragm is varied according to applied electrical power. For a given bias current, the quiescent temperature increase of the diaphragm is given by

$$\Delta T = \frac{I_S^2 R_S + I_H^2 R_H}{G_{th} - (I_S^2 R_S + I_H^2 R_H)\alpha} \tag{2}$$

where  $I_H$  and  $I_S$  are bias currents of a heater and a sensor, respectively,  $R_H$  and  $R_S$  the resistance values of a heater and a sensor, respectively, and  $\alpha$  the TCR of the sensor resistor. Bias currents of the heating and sensing resistors must be determined from electromigration limit, power consumption requirement and temperature limit of the electrothermal structure.

Fig. 6 shows schematic diagrams comparing a simple Gm-C integrator with an electrothermal integrator using the thermal structure. The ideal integrator should have a pole located at zero frequency. However, non-zero  $G_{th}$  of the electrothermal structure makes the integrator characteristics deviate from the ideal case. This non-zero pole location of the integrator introduces distortions in the overall filter transfer characteristics.

Let us take a look at filter characteristics in more details. The input signal applied to the structure is converted to a temperature signal by resistive heating power. This power is proportional to the square of the applied input current; therefore, the electrothermal integrator has non-linear transfer characteristics. If the power variation by the input ac signal ( $i_h$ ) is relatively smaller than the quiescent power, the relationship between the input electrical signal and power conversion can be approximately linearized as follows:

$$\delta\phi = 2I_H R_H i_h = \frac{2\phi_H}{I_H i_h} \tag{3}$$

where  $\delta\phi$  is the ac power signal  $i_h$  the input ac current and  $\phi_H$  the bias power of the heating resistor. The second-order

harmonic distortion ( $HD_2$ ) is given by

$$HD_2 = \frac{i_h}{4I_H}. \quad (4)$$

The quantity  $2I_H R_H$  or  $2\phi_H/I_H$  can be viewed as a power conversion gain. If a high conversion gain is required, a large heating resistor or a smaller bias current can be used for a given bias power consumption. The temperature variation of the diaphragm can be detected by resistance variation in the sensor resistor. This relation can be represented by

$$v = I_S \Delta R = I_S \alpha \Delta T R_S. \quad (5)$$

If we use identical heating and sensing resistors ( $R = R_H = R_S$ ) and the same bias current ( $I_B = I_H = I_S$ ), the unity gain frequency of the integrator is given by

$$\omega_T = \frac{2\alpha I_B^2 R^2 g_m}{C_{th}}. \quad (6)$$

In the filter design, characteristic frequencies, such as cut-off frequency in low-pass filters and center frequency in band-pass filters, should be near  $\omega_T$ . The characteristic frequencies can be tuned by various parameters such as bias current, transconductance, resistance value, thermal capacitance and TCR. It would be desirable that tuning procedure can be performed by customizing electrical parameters rather than thermal ones. In addition,  $\omega_T$  can be represented by other parameters as follows:

$$\omega_T = \frac{\alpha \phi_B R g_m}{C_{th}} = \frac{\alpha G_{th} \Delta T R g_m}{C_{th}} = \alpha \omega_P \Delta T R g_m \quad (7)$$

where  $\omega_P$  is the pole of the electrothermal structure. These equations for the unity gain frequency give us additional understandings. As discussed previously, non-zero pole of the integrator results in the distortion in the transfer function. This distortion can be specified as a phase error given by

$$\varphi_{error} = 90^\circ - \tan^{-1} \left( \frac{\omega_T}{\omega_P} \right) \quad (8)$$

where  $\omega_P = G_{th}/C_{th}$ . If  $\omega_T \geq 100\omega_P$ , the phase error will be less than  $0.5^\circ$ . For a given phase error, the minimum  $g_m$  can be determined by

$$g_{m \min} = \frac{\omega_T}{\alpha \omega_P \Delta T R}. \quad (9)$$

This is the minimum value of  $g_m$  that should be used in the circuit to guarantee the given phase error specification. For example, assuming that  $\omega_T = 100\omega_P$ ,  $\Delta T = 30^\circ\text{C}$ ,  $R = 5 \text{ k}\Omega$  and  $\alpha = 0.2\%/K$ , the required minimum  $g_m$  will be about  $300 \text{ mA/V}$ .

One of the important aspects that should be considered in the electrothermal filter design is signal dynamic range. The maximum variation in the sensor output voltage must be large enough to meet the required dynamic range. Let the maximum variation of the sensor output voltage be  $V_{\max}$ . The heater driving circuitry must provide the current that

makes sensor voltage swing up to  $V_{\max}$  at  $\omega_T$ . Therefore,

$$2I_B R i_{\max} = \omega_T C_{th} \delta T \quad (10)$$

$$V_{\max} = \frac{2\alpha I_B^2 R^2 i_{\max}}{\omega_T C_{th}}. \quad (11)$$

Substituting Eq. (6) into Eq. (11) gives

$$i_{\max} = g_{m \max} V_{\max}. \quad (12)$$

In the filter design,  $V_{\max}$  must be large enough to meet the dynamic range requirement. Because  $i_{\max}$  cannot exceed the bias current ( $I_B$ ),  $g_m$  should have an upper limit. In addition, it should be noted that large  $i_{\max}$  causes harmonic distortion. This  $g_m$  restriction is due to the quiescent bias operation of the electrothermal structure. From Eqs. (4) and (12), the maximum  $g_m$  can be found as  $4HD_2 I_B / V_{\max}$ . If we express it using  $G_{th}$  and quiescent temperature  $\Delta T$  instead of  $I_B$ ,  $g_{m \max}$  is given by

$$g_{m \max} = \frac{4HD_2}{V_{\max}} \sqrt{\frac{G_{th} \Delta T}{2R}}. \quad (13)$$

From the minimum and maximum restrictions imposed on  $g_m$ , the tunable range of  $\omega_T$  can be determined. The minimum tunable  $\omega_T$  is given by the phase error and  $\omega_P$  as follows:

$$\omega_{T \min} = \omega_P \tan(90^\circ - \varphi_{error}). \quad (14)$$

The maximum tunable  $\omega_T$  can be calculated by substituting Eq. (13) into Eq. (7):

$$\omega_{T \max} = \alpha \omega_P \Delta T \frac{HD_2}{V_{\max}} \sqrt{8G_{th} R \Delta T}. \quad (15)$$

Based on the previous discussions, electrothermal filter design procedure can be summarized as follows. From Eq. (12), it is desirable that  $g_m$  is maintained as small as possible for a large dynamic range and low power consumption. The minimum  $g_m$  value at a given phase error specification is given by Eq. (9). Next,  $I_B$  should be determined.  $I_B$  should be larger than  $i_{\max}$  and be suitable for a given  $HD_2$ . It is highly desirable that differential circuits should be employed for canceling out even harmonic distortions. Also,  $I_B$  should not be larger than electromigration limit. Even if the electromigration limit is satisfied, the quiescent power, approximately given by  $2I_B^2 R$ , should be carefully reviewed. The electrothermal structure should not cause thermal runaway or excess temperature rise at this bias of  $I_B$ . Note that the electrothermal structure should have  $C_{th}$  which is large enough to guarantee that  $\omega_P \ll \omega_T$ . Finally, when all above requirements are met,  $\omega_T$  can be tuned in the range given by Eqs. (14) and (15).

## 5. Experiments

The basic circuitry for electrically configurable filters is shown in Fig. 7. This circuit is adapted from the Gm-C filter scheme [7]. Differential circuit technique is employed to

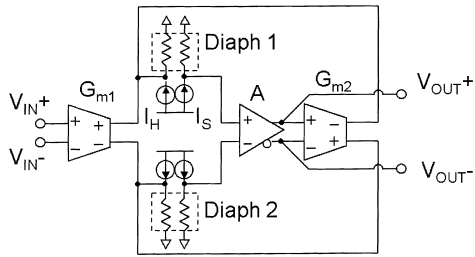


Fig. 7. Schematic diagram of basic filter block.

reduce the even harmonic distortion. The transfer function of the circuit is given by

$$H(s) = \frac{2\alpha A I_S I_H R_S R_H G_{m1}}{sC_{th} + (2\alpha A I_S I_H R_S R_H G_{m2} + G_{th})} \quad (16)$$

This circuit forms a first-order low-pass filter and is electrically tunable by properly adjusting transconductances ( $G_{m1}$ ,  $G_{m2}$ ), amplifier gain ( $A$ ), or bias currents ( $I_H$ ,  $I_S$ ) as denoted in the equation. As shown in Fig. 8, are measured responses of the filter when transconductance is varied to tune cut-off frequencies ranging from 30 to 300 Hz with  $A = 100$ .

The second-order filter characteristics has been tested using bi-quad connection of the basic blocks as shown in Fig. 9. Fig. 10 shows measured band-pass transfer

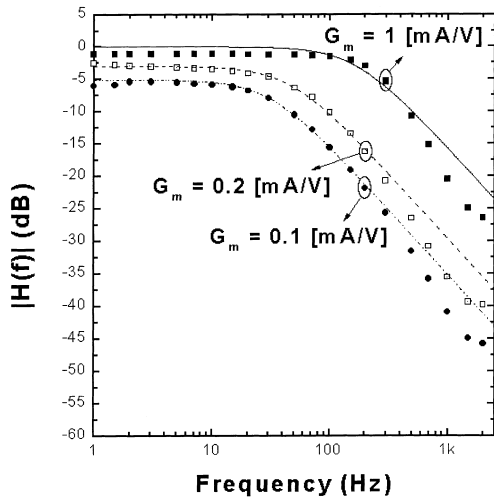


Fig. 8. Frequency responses of the first-order low-pass electrothermal filter.

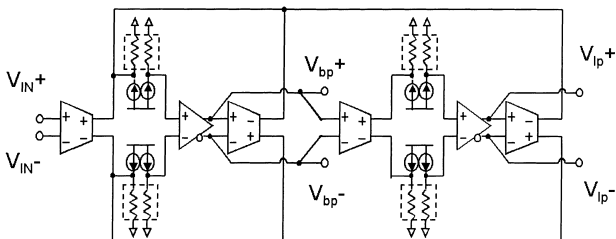


Fig. 9. Schematic diagram of the second-order electrothermal filter.

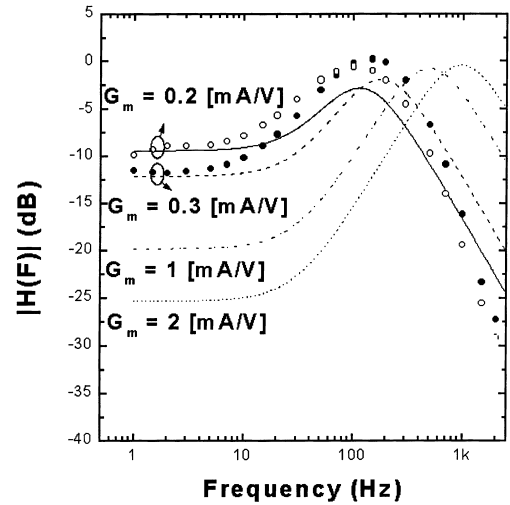


Fig. 10. Frequency response of the second-order band-pass electrothermal filter.

characteristics. The center frequency of the BPFs can be tuned in the similar way up to 300 Hz. In this case,  $\omega_T/\omega_P$  is not sufficiently high enough to tune the whole audio frequency range. This is why, Fig. 7 shows seriously-degenerated transfer characteristics.

### 6. Discussions

In this section, tunable frequency ranges of the electrothermal filter will be discussed. The tunable frequencies can be determined by the thermal conductance ( $G_{th}$ ) and thermal time constant (or  $\omega_p$ ) of the structure as well as the TCR of the sensing material. Fig. 11 shows the minimum required thermal conductance for the electrothermal filter tuned to  $f_T$  where,  $f_T = \omega_T/2\pi$ . This plot shows two possible materials for sensing resistors [4,8]. Nickel resistors have a typical TCR of about 0.24% while vanadium oxide resistors have that of about 2%. If  $f_T$  forms near at 100 Hz, the pole of

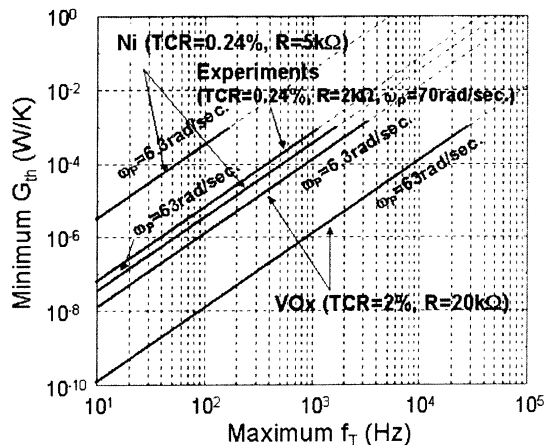


Fig. 11. Minimum required thermal conductance ( $G_{th}$ ) corresponding to  $f_T$ .

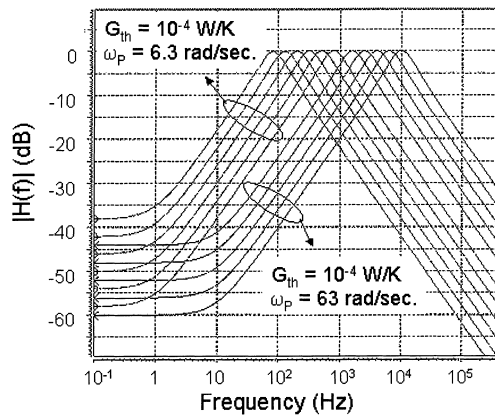


Fig. 12. Simulated second-order BPF characteristics using the material with a high TCR of 2%.

electrothermal structure,  $\omega_T$ , should be below 6.3 rad/s for  $< 0.5^\circ$  phase error. It is assumed that  $\Delta T = 20$  K and  $V_{\max} = 2$  mV for a dynamic range of 60 dB with thermal noise at 10 kHz bandwidth. As this plot shows, Nickel resistors of  $\omega_p = 6.3$  rad/s is hard to be used to tune above 100 Hz because of electromigration limit (a few mA) and excess power consumption (above 10 mW).

Electrothermal structures using a high TCR material (e.g. vanadium oxide) are expected to be more suitable elements for audio frequency filter design [9]. This is mainly due to the high TCR value. Fig. 12 shows the simulated BPF characteristics assuming that the TCR of the resistors in the electrothermal structure is 2%. For the frequency ranges from 100 Hz to 1 kHz and from 1 to 10 kHz, two different diaphragms of  $\omega_p = 6.3$  and 63 rad/s have been used for simulations, respectively. This is because it is more desirable to use the structure with a high  $\omega_p$  for tuning the filter in the high frequency range to reduce power consumption. Simulation results show that about 2 mW quiescent power is dissipated per each thermal structure. Transconductances have been tuned in the range of 10–100 mA/V in the entire audio frequency ranges.

## 7. Conclusions

We have demonstrated the electrothermal filter applications of the thermally-isolated diaphragm structures. Low-pass and band-pass electrothermal filters have been fabricated, tested and tuned from 30 to 300 Hz. It has been suggested from the simulations that electrothermal filters can be realized in the audio frequency range (from 100 Hz to 10 kHz) when the materials with a TCR higher than 2%/K are used for the resistors in the thermal structure. These electrothermal filters can be applied to audio band filter applications such as implementation of basilar membrane models and loop filters in the automatic adaptation technique.

## Acknowledgements

This work has been partially supported by the G7 project from Ministry of Industry and Energy and Ministry of Science and Technology of Korea, and partially supported by Brain Science Research Center at KAIST.

## References

- [1] E. Yoon, K.D. Wise, An integrated mass flow sensor with on-chip CMOS interface circuitry, *IEEE Trans. Electron Devices* (1992) 1376–1386.
- [2] E. Yoon, K.D. Wise, A wideband monolithic rms-dc converter using micromachined diaphragm structures, *IEEE Trans. Electron Devices*, (1994) 1666–1668.
- [3] P.E. Eriksson, J.Y. Andersson, G. Stemme, Thermal characterization of surface-micromachined silicon nitride membranes for thermal infrared detectors, *IEEE J. Microelectromech. Syst.* (1997) 55–61.
- [4] H.K. Lee, J.B. Yoon, E. Yoon, S.B. Ju, Y.J. Yong, W. Lee, S.G. Kim, A high fill-factor infrared bolometer using micromachined multilevel electrothermal structures, *IEEE Trans. Electron Devices* (1999) 1489–1491.
- [5] P.R. Gray, D.J. Hamilton, Analysis of electrothermal integrated circuits, *IEEE J. Solid-State Circuits* (1971) 8–14.
- [6] W.J. Louw, D.J. Hamilton, W.J. Kerwin, Inductor-less, capacitor-less state-variable electrothermal filters, *IEEE J. Solid-State Circuits* (1977) 416–423.
- [7] R. Schaumann, Continuous-time integrated filters — a tutorial, *IEE Proc.* (1989) 184–190.
- [8] B.E. Cole, R.E. Higashi, R.A. Wood, Monolithic two-dimensional arrays of micromachined microstructures for infrared applications, *Proc. IEEE* (1998) 1679–1698.
- [9] K. Lee, H. Byun, H. Lee, I. Cho, J. Bu, E. Yoon, An Audio Frequency Filter Application of Micromachined Thermally-Isolated Diaphragm Structure, in: *Proceedings of the IEEE MEMS 2000 Conference*, January 2000, pp. 142–147.

## Biographies

*Kwang-Hyun Lee* was born in Seoul, Korea, on 9 June, 1974. He received the BS degree in Electrical Engineering from Korea Advanced Institute of Science and Technology (KAIST), Taejeon, Korea, in 1997 and MS degree in Electrical Engineering from the same institute on the subject of CMOS readout circuit design for an uncooled infrared micro-bolometer array in 1999, respectively. Since then, he has been working towards the PhD degree at the same institute. His current research interests include sensor readout circuit design, CMOS image sensor design, and VLSI systems.

*Hyung-Kew Lee* received the BS and the MS degrees in Electrical Engineering from Korea Advanced Institute of Science and Technology (KAIST), Taejeon, Korea, in 1997 and 1999, respectively. He has worked on uncooled infrared micro-bolometers. He is currently pursuing the PhD degree at the same university. His research interests are optical network components and biomedical components using MEMS technology.

*Il-Joo Cho* received the BS and MS degrees in Electrical Engineering from Korea Advanced Institute of Science and Technology (KAIST), Taejeon, Korea, in 1998 and 2000, respectively. Since then, he is working as the PhD candidate student at the same institute. His current research interests are in the atomic force microscopic devices and micro-lens for optical storage devices.

*Euisik Yoon* received the BS and MS degrees in Electronics Engineering from Seoul National University in 1982 and 1984, respectively, and PhD degree in Electrical Engineering from the University of Michigan, Ann Arbor, in 1990. From 1990 to 1994 he was with the Fairchild Research Center of the National Semiconductor Corp., Santa Clara, CA, where he was engaged in researches on deep submicron CMOS integration and advanced gate dielectrics. From 1994 to 1996 he was a Member of

Technical Staff at Silicon Graphics Inc., Mountain View, CA, working on the design of the MIPS microprocessor R4300i and the RCP 3-D graphic coprocessor. In 1996, he joined the Department of Electrical Engineering at Korea Advanced Institute of Science and Technology (KAIST), Taejon, Korea, where he is currently an assistant professor. His present research interests are in microsensors, integrated microsystems, and VLSI circuit design.